

# Theoretical Study of the Stable Radicals Galvinoxyl, Azagalvinoxyl and Wurster's Blue Perchlorate in the Solid State

Remco W. A. Havenith,<sup>†</sup> Gilles A. de Wijs,<sup>†</sup> Jisk J. Attema,<sup>†</sup> Natascha Niermann,<sup>‡</sup> Sylvia Speller,<sup>‡</sup> and Robert A. de Groot<sup>\*,†,§</sup>

*Electronic Structure of Materials, Institute for Molecules and Materials, Radboud University Nijmegen, Heyendaalseweg 135, 6525 AJ Nijmegen, The Netherlands, Scanning Probe Microscopy, Institute for Molecules and Materials, Radboud University Nijmegen, Heyendaalseweg 135, 6525 AJ Nijmegen, The Netherlands, and Chemical Physics, Zernike Institute for Advanced Materials, University of Groningen, Nijenborgh 4, 9747 AG Groningen, The Netherlands*

Received: March 6, 2008; Revised Manuscript Received: June 14, 2008

Calculations on crystalline organic radicals were performed to establish the ground states of these materials. These calculations show that the radicals may interact, depending on their orientation in the crystal structure. For galvinoxyl, a second structure is proposed which is similar to that of azagalvinoxyl, in which the radicals form pairs. This structure accounts for the anomalous magnetic properties of galvinoxyl at low temperatures.

## 1. Introduction

Stable radicals such as the galvinoxyl radical (**1**), azagalvinoxyl (**2**), and the *N,N,N',N'*-tetramethyl-*p*-diaminobenzene radical cation (**3**) (Scheme 1) have attracted interest for their magnetic properties. Electron spin resonance (ESR) measurements of crystalline galvinoxyl (**1**) at different temperatures<sup>1–3</sup> revealed that above 85 K a so-called ferromagnetic phase exists, and at 85 K a phase transition occurs to an antiferromagnetic phase, accompanied by pairing of the spins and concomitantly a decrease in paramagnetism and broadening and decrease of ESR signal. Scanning tunnelling microscopy (STM) measurements on monolayers of galvinoxyl, deposited on a gold [Au(111)] surface, also showed that two different configurations could be formed.<sup>4</sup> One phase is similar to the crystal structure of galvinoxyl, and a second configuration, which was formed after cooling down to 40 K and going back to room temperature, gave distinctly brighter spots in the STM image. These results suggest that a phase transition similar to that in the solid state can also occur on gold in a two-dimensional aggregate layer.

The galvinoxyl (**1**) radical is not unique in its magnetic behavior in the solid state: similar observations were made for the perchlorate salt of **3**: two different crystal structures could be determined and, concomitantly with the phase transition to the low-temperature structure around 190 K, a decrease in spin concentration was observed.<sup>5–9</sup>

Several mechanisms have been proposed to account for this behavior, e.g., the disproportionation of  $3^{+\bullet}$  into  $3^{2+}$  and **3**,<sup>10</sup> and dimer formation.<sup>6</sup> Elucidation of the crystal structure of the low-temperature phase<sup>11</sup> ruled out the “mol-ionic” lattice formed by  $3^{2+}$  and **3**.

In the case of galvinoxyl, dimer formation along the *c*-axis of the crystal has been put forward to explain the change in magnetism and disappearance of the ESR signal.<sup>1</sup> Unfortunately, only the high-temperature crystal structure has been determined

so far,<sup>12</sup> as disintegration of the crystals at the phase transition temperature prevented the crystal structure analysis at lower temperatures.<sup>13</sup> However, a radical dimer with a singlet ground state has been observed in the solid state for the isoelectronic nitrogen analogue of galvinoxyl, azagalvinoxyl (**2**).<sup>14</sup> A distinct difference between the crystal structure of **1** and that of **2** is that the phenyl rings of **1** are nearly coplanar, and those of **2** are twisted by 47° with respect to each other.

Using temperature-dependent ESR measurements in solution, dimerization enthalpies ( $\Delta H_{\text{dim}}$ ) for **1** and **3** have been determined.<sup>15</sup>  $\Delta H_{\text{dim}} = -529$  meV ( $-51.0$  kJ/mol) and  $-307$  meV ( $-29.6$  kJ/mol) were found for **1** and **3**, respectively, but the dimerization products were not identified. The conclusion that dimerization had taken place was based on the change of the ESR intensity as a function of temperature.

On both **1** and **3** calculations have been performed,<sup>16–19</sup> and spin-interaction models have been proposed to rationalize the magnetic behavior of these compounds.<sup>10,16–22</sup> An important outcome of these studies is that the stacking of the molecules determines the ferro- or antiferromagnetic interaction between the molecules<sup>17</sup> in 1D crystals. GGA calculations on the high-temperature crystal structure of galvinoxyl (**1**) led to the conclusion that **1** has a ferromagnetic ground state.<sup>18</sup>

Here, we report calculations on the high- and low-temperature phases of Wurster's blue perchlorate (**3**), on the crystal structure of azagalvinoxyl (**2**) and galvinoxyl (**1**), backed up by calculations on molecular models for crystalline galvinoxyl. On the basis of these calculations, we propose a second structure for galvinoxyl (**1**) in which an interaction between the radicals exists. The calculations confirm the earlier propositions that the intermolecular interaction, which governs the ground state, depends on the stacking of the molecules. The proposed second crystal structure of galvinoxyl (**1**) explains the disappearance of the ESR signal.

## 2. Computational Details

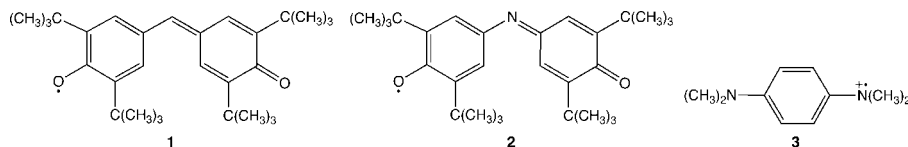
The solid state DFT calculations were performed with the Vienna Ab Initio Simulation Package (VASP),<sup>23,24</sup> using the projector augmented-wave method,<sup>25,26</sup> and a GGA extension of the local spin density approach (LSDA). The chosen exchange–correlation

\* Corresponding author. E-mail: R.deGroot@science.ru.nl.

<sup>†</sup> Electronic Structure of Materials, Institute for Molecules and Materials, Radboud University of Nijmegen.

<sup>‡</sup> Scanning Probe Microscopy, Institute for Molecules and Materials, Radboud University of Nijmegen.

<sup>§</sup> University of Groningen.

**SCHEME 1: Structure of Galvinoxyl (1), Azagalvinoxyl (2), and the  $N,N,N',N'$ -Tetramethyl- $p$ -phenylenediamine Cation (3)**


functional was PBE.<sup>27</sup> The basis set consisted of plane-waves, the cutoff energy was 400 eV, and the augmentation cutoff energy was 645 eV. The calculations on Wurster's blue perchlorate (3) and azagalvinoxyl (2) were performed on their experimentally determined crystal structures, with  $k$ -points chosen on a  $5 \times 5 \times 5$   $\Gamma$ -centered Monkhorst–Pack grid. For galvinoxyl (1), the first structure was determined by optimization of the ion positions starting from their experimental ones, while keeping the cell parameters fixed. The second configuration was determined by optimization of both ion positions and cell parameters; all were derived from the experimental positions of azagalvinoxyl (2). Both optimizations for 1 were performed at the  $\Gamma$ -point only; for the final energy calculations, a  $5 \times 5 \times 5$   $\Gamma$ -centered Monkhorst–Pack grid was used.

The calculations on the molecular models (see text) were performed using GAMESS-UK<sup>28</sup> (PBE/6-31G\* geometry optimizations, PBE/6-31G\*\*//PBE/6-31G\* single point, and restricted open-shell RMP2 calculations), Dalton<sup>29</sup> (CCSD calculations), and Gaussian03<sup>30</sup> (unrestricted open-shell UMP2, and UMP4, and unrestricted UCCSD calculations). The frozen-core approximation was used in the MP2 and MP4(SDQ) calculations (15/30 for the monomer/dimer); in the CCSD calculations the first 28 orbitals were frozen for the monomer and 54 orbitals for the dimer.

### 3. Results

**3.1. Wurster's Blue Perchlorate (3).** We start our discussion with the results of our calculations on Wurster's blue perchlorate (3), because for this compound both high- (HT) and low-temperature (LT) crystal structures have been determined.<sup>11,31</sup> The stacking of the molecules in HT and LT phases differs substantially (Figure 1). The nitrogen atom of one molecule of 3 aligns itself above a carbon atom of a second molecule, and the intermolecular distance decreases upon going to the low-temperature phase from 3.6 to 3.3 Å.

According to the calculated energies, for the high-temperature phase (Table 1) the ferromagnetic state ( $\uparrow\uparrow$ ) has almost the same energy as the antiferromagnetic state ( $\uparrow\downarrow$ ) (relative spin as indicated for the dimers in the Figure). This degeneracy and the distance of the radicals in the crystal (Figure 1) indicate that the molecules do not interact strongly. The low-temperature

**TABLE 1: PBE Results for 3 in the High-Temperature, Ferromagnetic State (HT-( $\uparrow\uparrow$ )), High-Temperature, Antiferromagnetic State (HT-( $\uparrow\downarrow$ )), Low-Temperature, Ferromagnetic State (LT-( $\uparrow\uparrow$ )), and Low-Temperature, Antiferromagnetic State (LT-( $\uparrow\downarrow$ ))<sup>a</sup>**

crystal structure/state	energy (eV)	$\Delta E_{[\uparrow\downarrow]-[\uparrow\uparrow]}$	$E_{\text{rel}}$
HT-( $\uparrow\uparrow$ )( $Z=2$ )	-354.1157	0.2	116.4
HT-( $\uparrow\downarrow$ )( $Z=2$ )	-354.1154		116.5
LT-( $\uparrow\uparrow$ )( $Z=4$ )	-708.6353	-15.4	15.4
LT-( $\uparrow\downarrow$ )( $Z=4$ )	-708.6969		0.0

<sup>a</sup>  $Z$  denotes the number of molecules in the unit cell.  $\Delta E_{[\uparrow\downarrow]-[\uparrow\uparrow]}$  and  $E_{\text{rel}}$  in meV/molecule-3.

phase is more stable than the high-temperature phase (Table 1), and in this phase, the ( $\uparrow\downarrow$ ) state is significantly lower in energy than the ( $\uparrow\uparrow$ ) state. This can be rationalized by the shorter intermolecular distance (Figure 1), so that the nitrogen and carbon  $p$ -orbitals of two  $3^{+\cdot}$  molecules can overlap and interact, which results in a preference for the antiferromagnetic ( $\uparrow\downarrow$ ) state as the ground state. The energy difference between the ( $\uparrow\downarrow$ ) and ( $\uparrow\uparrow$ ) state is still small (Table 1), and thus the ( $\uparrow\uparrow$ ) excited state can be populated thermally.

**3.2. Azagalvinoxyl (2).** For azagalvinoxyl (2), one crystal structure is known (Figure 2), measured at 193 K.<sup>14</sup> The magnetic susceptibility measurements<sup>32</sup> suggest a singlet ground state, which is confirmed by our PBE calculations (Table 2). The antiferromagnetic state is 134.1 meV/molecule-2 more stable than the ferromagnetic state. The interaction between the azagalvinoxyl is caused by the overlap of the  $p$ -orbitals on the carbon atoms in the phenyl rings, as indicated in Figure 2 by the solid line. The two molecules cannot form a real bond, presumably due to the steric hindrance of the *tert*-butyl groups. This crystal structure may serve as a starting point for the search to an antiferromagnetic galvinoxyl (1) phase.

**3.3. Galvinoxyl (1).** The results of the calculations on the experimental crystal structure (with unit-cell parameters  $a = b = 13.07$  Å,  $c = 23.12$  Å,  $\alpha = \beta = 144.6^\circ$ , and  $\gamma = 49.1^\circ$ )<sup>12</sup> for the ferro- ( $\uparrow\uparrow$ ) and antiferromagnetic ( $\uparrow\downarrow$ ) state (Table 3) show that both states have nearly identical energies, and that the ferromagnetic state is slightly favored. These calculations are inline with previously reported results.<sup>18</sup> The distance between

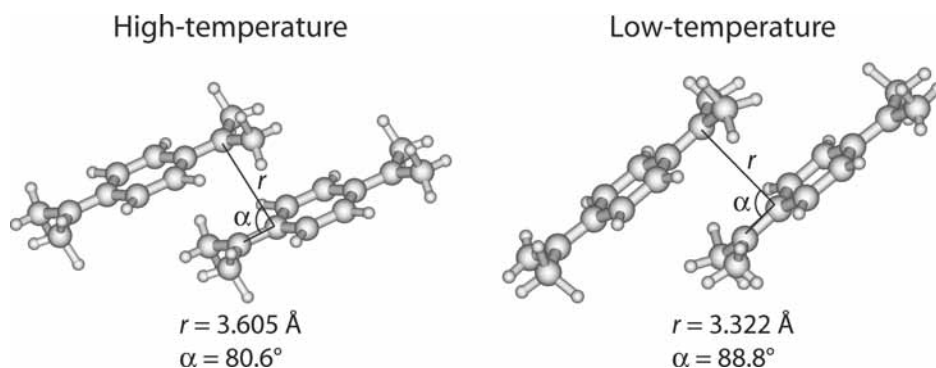


**Figure 1.** Stacking of two molecules in the experimental high- and low-temperature phases of  $3^{+\cdot}\text{ClO}_4^-$ .

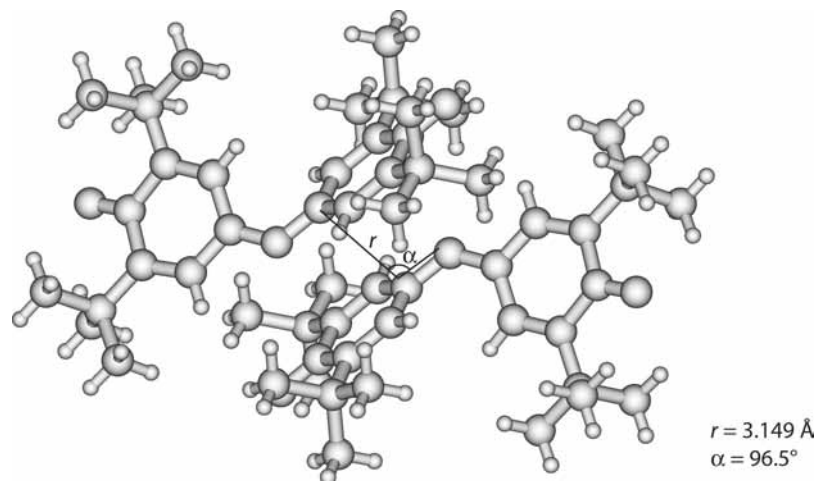


**Figure 2.** Azagalvinoxyl (**2**) dimer as found in the crystal structure.

**TABLE 2: PBE Results for **2** in the Ferromagnetic State [(↑↑)] and Antiferromagnetic State [(↑↓)]<sup>a</sup>**

state	energy (eV)	$\Delta E_{[(\uparrow\downarrow)-(\uparrow\uparrow)]}$
(↑↑) ( $Z = 2$ )	-803.0833	-134.1
(↑↓) ( $Z = 2$ )	-803.2174	

<sup>a</sup>  $Z$  denotes the number of molecules in the unit cell.  $\Delta E_{[(\uparrow\downarrow)-(\uparrow\uparrow)]}$  in meV/molecule-2.

**TABLE 3: PBE Results for **1** in the High-Temperature, Ferromagnetic State (HT-(↑↑)), High-Temperature, Antiferromagnetic State (HT-(↑↓)), Proposed Low-Temperature, Ferromagnetic State (LT-(↑↑)), and Proposed Low-Temperature, Antiferromagnetic State (LT-(↑↓))<sup>a</sup>**

crystal structure/state	energy (eV)	$\Delta E_{[(\uparrow\downarrow)-(\uparrow\uparrow)]}$	$E_{\text{rel}}$
HT-(↑↑) ( $Z = 2$ )	-851.5477	1.3	0.0
HT-(↑↓) ( $Z = 2$ )	-851.5451		1.3
LT-(↑↑) ( $Z = 2$ )	-850.6303	-46.1	458.7
LT-(↑↓) ( $Z = 2$ )	-850.7225		412.6

<sup>a</sup>  $Z$  denotes the number of molecules in the unit cell.  $\Delta E_{[(\uparrow\downarrow)-(\uparrow\uparrow)]}$  and  $E_{\text{rel}}$  in meV/molecule-1.

two carbon atoms of different molecules is larger than 4 Å (Figure 3a), suggesting that the molecules do not interact strongly, which is confirmed by the near-degeneracy of the (↑↓) and (↑↑) states.

The unpaired electron is delocalized over the molecule, as the spin-population on the atoms suggests: both oxygen atoms

**SCHEME 2: Model Dimerization Reaction**

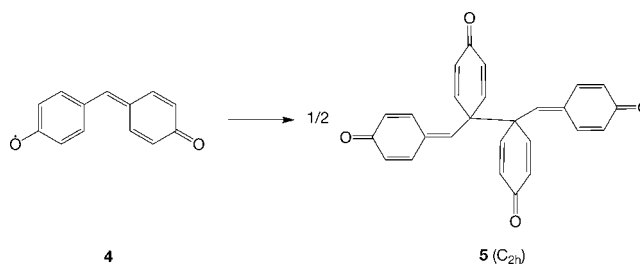


**TABLE 4: Ab Initio Results for the Reaction  $4 \rightarrow \frac{1}{2}5$  (Scheme 2), Calculated Using the PBE/6-31G\* Optimized Geometry<sup>a</sup>**

method	$E(4)$	$E(5)$	$\Delta E$ (mH)	$\Delta E$ (meV)
PBE/6-31G**	-650.4133185	-1300.8028041	11.9	324.3
UMP2/6-31G**	-649.1318434	-1298.4948802	-115.6	-3145.6
RMP2/6-31G**	-649.2466021	-1298.4948802	-0.8	-22.8
UMP4(SDQ)/6-31G**	-649.2354987	-1298.5867356	-57.9	-1574.7
UCCSD/6-31G**	-648.3805253	-1296.7767048	-7.8	-213.0

<sup>a</sup> Total energies of **4** and **5** are in Hartree, and the energy differences are in mHartree/molecule-4 and meV/molecule-4.

possess a spin-population of 0.13 electron, and on the carbon atoms of the phenyl rings, an alternating spin-population starting from C=O of 0.00, 0.07, -0.03, 0.10, and -0.04 electron is found.

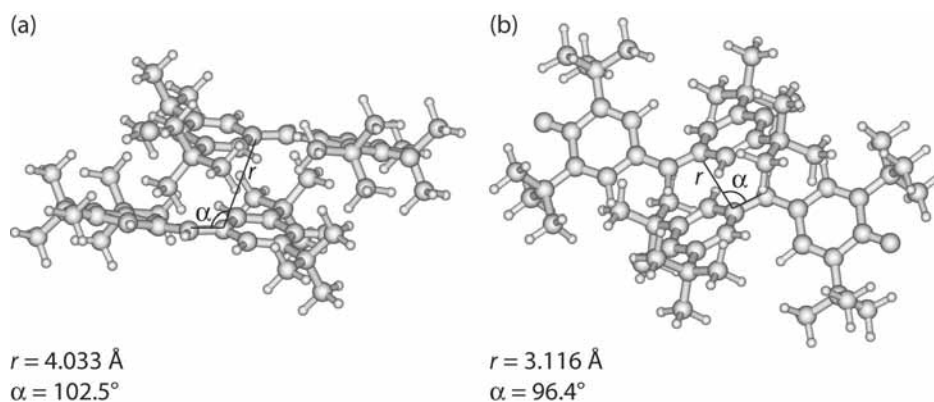


**Figure 3.** Two molecules from (a) the optimized crystal structure of galvinoxyl as determined starting from the experimental structure and (b) the optimized crystal structure as determined starting from a structure similar to that of azagalvinoxyl (**2**).

**TABLE 5: Ab Initio Results for the Energy Difference Per Model Galvinoxyl (4) Molecule between the Dimers of 4 in the HT and LT Structures<sup>a</sup>**

method	4-HT	4-LT	$\Delta E$ (mH)	$\Delta E$ (meV)
PBE/6-31G**	-1300.8196974	-1300.8129746	3.4	91.5
GVB-1/6-31G**	-1294.3516079	-1294.3443012	3.7	99.4
CASPT2/6-31G**	-1298.6052508	-1298.6134285	-4.1	-111.3

<sup>a</sup> Total energies are in Hartree, and the energy differences are in mHartree/molecule-4 and meV/molecule-4.

**TABLE 6: Total Energies (Hartree) Obtained for the Cations and Anions of 4-HT and 4-LT at the PBE/6-31G\*\* Level of Theory, and Their Ionization Potentials (IP) and Electron Affinities (EA) (eV)**

dimer	$E_{\text{cation}}$ (au)	$E_{\text{anion}}$ (au)	IP (eV)	EA (eV)
4-HT	-1300.5645142	-1300.9426193	6.94	-3.35
4-LT	-1300.5571135	-1300.9377074	6.96	-3.67

Optimization starting from a structure derived from that of azagalvinoxyl (2) resulted in a second crystal structure for galvinoxyl (2). In this structure, the galvinoxyl molecules form pairs (Figure 3b). The carbon-carbon distance falls to 3.1 Å, and the two atoms approach to an on-top placing. The galvinoxyl molecule itself becomes more twisted: the twist angle between the two phenyl rings increases from 17.3° to 40.3°. The unit-cell parameters change considerably in the proposed LT-structure from  $a = b = 13.07$  Å,  $c = 23.12$  Å,  $\alpha = \beta = 144.6^\circ$ , and  $\gamma = 49.1^\circ$ <sup>12</sup> for the HT-structure to  $a = 10.5$  Å,  $b = 12.2$  Å,  $c = 10.1$  Å,  $\alpha = 101.7^\circ$ ,  $\beta = 92.8^\circ$ , and  $\gamma = 98.8^\circ$ .

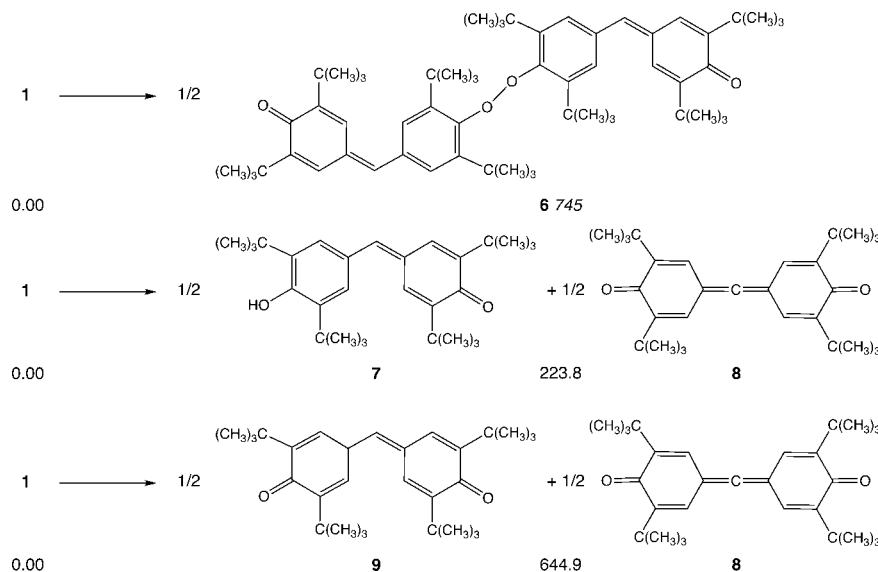
The energy difference between the ( $\uparrow\downarrow$ )- and ( $\uparrow\uparrow$ )-spin-couplings is 46.1 meV/molecule-1, in favor of the ( $\uparrow\downarrow$ ) state. If this crystal structure were formed at low temperatures, then the ground state of the galvinoxyl crystal would be ESR silent; the higher lying excited ferromagnetic state could be thermally populated, and might be observed in an ESR experiment.

The spin populations on the phenyl carbon atoms are still alternating: for the phenyl ring that forms the dimer, they vary from C=O 0.00, 0.05, -0.02, 0.08, -0.04 electron, and on the oxygen atom the spin population is 0.11 electron. The spin

population on oxygen connected to the other phenyl ring is slightly lower (0.08 electron). In comparison with the spin population obtained for the experimental crystal structure, these values are only slightly reduced.

The energy of the HT structure is, according to the PBE calculations, significantly lower than that of the proposed LT structure (412.6 meV/molecule-1, Table 3). This energy difference is large enough that it seems that the proposed LT structure cannot be formed at low temperatures. However, the accuracy of this energy difference calculated at the PBE level is questionable, as shown by calculations on the dimerization reaction of 4 (model for galvinoxyl with the *tert*-butyl groups replaced by hydrogen) to  $1/2$ 5 (dimerization product that is formed when the two radical carbon centers that interact in the proposed LT solid state structure (Figure 3b) have formed a bond, Scheme 2). At the PBE/6-31G\*\*//PBE/6-31G\* level of theory, an energy difference of 324.3 meV/molecule-4 (Table 4) is obtained for this model reaction. As can be seen from Table 4, different theoretical treatments predict different dimerization energies. A considerable difference is found at the MP2 level depending on the zeroth-order treatment of 4 being RHF or UHF. In the latter case, severe spin contamination is found:  $\langle S^2 \rangle = 2.59$  as opposed to the expected value of 0.75. At the UMP4(SDQ)/6-31G\*\* level of theory, the dimerization energy is less exothermic than at the UMP2 level, but still a large discrepancy is found between calculated values and an experimentally determined dimerization enthalpy for galvinoxyl (1) of -264.3 meV/molecule-1.<sup>15</sup> The coupled cluster dimerization energy of -213.0 meV/molecule-4 is closer to this experimental value. Thus, it can be concluded that the stability of 4 is overestimated by approximately 500 meV/molecule-4 at the PBE/6-31G\*\* level of theory. Therefore, a more elaborate theoretical treatment of 4 is required to obtain reliable dimerization energies, and a correct energy difference between the two crystal structures.

To further estimate the energy difference between the two different crystal structures, the energy difference between the dimers of model 4, one in a structure that matches that of 1 in the HT crystal structure and one in a structure that matches that of 1 in the proposed LT crystal structure, was determined at different levels of theory. The energy differences calculated at the PBE/6-31G\*\* and GVB-1/6-31G\*\* levels of theory have

**SCHEME 3: Peroxide (6) Formation and Decomposition Pathways of 1<sup>a</sup>**

<sup>a</sup> Reaction energies calculated at the PBE/6-31G\*\*//PBE/6-31G\* level of theory in meV per galvinoxyl (1) molecule. Note that 6 is not a stationary point at the PBE/6-31G\* potential energy surface (see text).

both the same magnitude and suggest that the formation of the dimer is energetically not favorable. They are significantly smaller than the solid state PBE energy difference of 412.6 meV/molecule-1. This is attributed to the steric hindrance of the *tert*-butyl groups in **1**. However, at the CASPT2/6-31G\*\* (CASSCF(2,2) reference wave function) level of theory, the dimerization process is slightly exothermic (Table 5). The difference between the PBE and CASPT2 treatments would suggest a relatively small correction of only 200 meV/molecule-4: however, we expect this value to be too small. Following the analogy in the model dimerization process where RMP2 (which is comparable to the CASPT2 treatment in this case) overestimates the stability of **4** (Table 4), the energy difference between **4-LT** and **4-HT** is expected to be larger at a higher level of theory.

According to the solid state calculations, the proposed LT-structure is 412.6 meV per galvinoxyl (**1**) molecule higher in energy than the HT structure (Table 3). If an ad hoc correction of 500 meV/molecule were applied to correct this energy difference for the overestimation of the stability of the galvinoxyl radical at the PBE level, the LT structure would be predicted to be 87.4 meV/molecule-1 lower than the HT structure. Thus, it can be concluded that the energy difference between the noninteracting monomer structure (**4-HT**) and the dimer structure (**4-LT**) is small, and that the formation of **4-LT** is energetically possible. It should be noted that, to get a more reliable estimate of this energy difference, higher-level calculations are required, which are not computationally feasible at this moment.

The ionization potentials and electron-affinities for both dimers have been calculated using the  $\Delta$ SCF approach at the PBE/6-31G\*\* level of theory (Table 6). The LT dimer has a higher electron affinity than the HT dimer, whereas the difference between the ionization potentials is negligibly small. This difference in electron affinity will be useful in the experimental verification of the formation of this crystal structure.

Other dimerization or decomposition processes such as formation of a peroxide or hydrogen abstraction, followed by allene and alcohol formation (Scheme 3) were also considered. However, geometry optimization of the peroxide dimer **6** failed at the PBE/6-31G\* level: elongation of the peroxide O–O bond occurred until the O–O bond distance reached 1.848 Å and the SCF calculation did not converge; the energy at this point is 745 meV/molecule-1 higher than that of galvinoxyl. The disproportionation of galvinoxyl in hydroxygalvinoxyl (**7**) and 4,4'-methanediylidene-bis(2,6-di-*tert*-butylcyclohexa-2,5-dienone) (**8**) (Scheme 3) via hydrogen transfer is energetically not favored. However, this reaction would become energetically possible, if a correction of 500 meV/molecule-1 is applied. Decomposition to 4,4'-methylenebis(2,6-di-*tert*-butylcyclohexa-2,5-dienone) (**9**) and **8** (Scheme 3) is less likely, even if the reaction energy is corrected for the overestimation of the stability of **1**. However, the reaction barriers for these hydrogen transfers are expected to be high, due to steric hindrance, and the reactions are expected to be slow, especially at low temperatures.

#### 4. Conclusions

Calculations on the crystal structures of some organic radicals revealed that these radicals can form pairs in the solid state in which the radical centers interact by direct overlap. For the galvinoxyl (**1**), a second structure is proposed, which resembles the crystal structure of azagalvinoxyl (**2**). In this structure, the galvinoxyl molecules form dimers, with a singlet spin-coupling as the ground state. This structure can account for the anomalous magnetic properties of galvinoxyl at low temperatures (viz. the disappearance of the ESR signal, and the sudden increase in diamagnetism).

**Acknowledgment.** We acknowledge Dr. P. J. M. van Bentum (Radboud University Nijmegen) for enlightening discussions considering ESR spectroscopy. This work is part of the research programme of the Stichting voor Fundamenteel Onderzoek der Materie (FOM), which is financially supported by the Nederlandse Organisatie voor Wetenschappelijk Onderzoek (NWO).

**Supporting Information Available:** Tables with the coordinates and lattice parameters of the two calculated galvinoxyl (**1**) crystal structures. This information is available free of charge via the Internet at <http://pubs.acs.org>.

#### References and Notes

- Mukai, K.; Sogabe, A. *J. Chem. Phys.* **1980**, *72*, 598.
- Mukai, K.; Ueda, K.; Ishizu, K. *J. Chem. Phys.* **1982**, *77*, 1606.
- Awaga, K.; Sugano, T.; Kinoshita, M. *Chem. Phys. Lett.* **1986**, *128*, 587.
- Niermann, N.; Hailu Degefa, T.; Walder, L.; Zielke, V.; Steinhoff, H.-J.; Onsgaard, J.; Speller, S. *Phys. Rev. B* **2006**, *74*, 235424.
- Duffy, W., Jr. *J. Chem. Phys.* **1961**, *36*, 90.
- Thomas, D. D.; Keller, H.; McConnell, H. M. *J. Chem. Phys.* **1963**, *39*, 2321.
- Pott, G. T.; Kommandeur, J. *J. Chem. Phys.* **1967**, *47*, 395.
- Pott, G. T.; van Bruggen, C. F.; Kommandeur, J. *J. Chem. Phys.* **1967**, *47*, 408.
- McConnell, H. M.; Pooley, D.; Bradbury, A. *Proc. Natl. Acad. Sci.* **1962**, *48*, 1480.
- Monkhorst, H. J.; Pott, G. T.; Kommandeur, J. *J. Chem. Phys.* **1967**, *47*, 401.
- de Boer, J. L.; Vos, A. *Acta Crystallogr.* **1972**, *B28*, 839.
- Williams, D. E. *Mol. Phys.* **1969**, *16*, 145.
- Chi, K.-M.; Calabrese, J. C.; Miller, J. S.; Khan, S. I. *Mol. Cryst. Liq. Cryst.* **1989**, *176*, 185.
- Chi, K.-M.; Calabrese, J. C.; Miller, J. S. *Mol. Cryst. Liq. Cryst.* **1989**, *176*, 173.
- Grampp, G.; Landgraf, S.; Rasmussen, K.; Strauss, S. *Spectrochim. Acta Part A* **2002**, *58*, 1219.
- Dietz, F.; Tyutyulkov, N.; Christen, C.; Lüders, K. *Chem. Phys. Lett.* **1997**, *218*, 43.
- Dietz, F.; Tyutyulkov, N.; Baumgarten, M. *J. Phys. Chem. B* **1998**, *102*, 3912.
- Luo, S. J.; Yao, K. L. *J. Magn. Magn. Mater.* **2003**, *257*, 11.
- Novak, I.; Kovač, B. *Chem. Phys. Lett.* **2005**, *413*, 351.
- McConnell, H. M.; Lynden-Bell, R. *J. Chem. Phys.* **1962**, *36*, 2393.
- Soos, Z. G.; Hughes, R. C. *J. Chem. Phys.* **1967**, *46*, 253.
- Kollmar, C.; Kahn, O. *J. Am. Chem. Soc.* **1991**, *113*, 7987.
- Kresse, G.; Hafner, J. *Phys. Rev. B* **1993**, *47*, 558.
- Kresse, G.; Furthmüller, J. *Phys. Rev. B* **1996**, *54*, 11169.
- Blöchl, P. E. *Phys. Rev. B* **1994**, *50*, 17953.
- Kresse, G.; Joubert, D. *Phys. Rev. B* **1999**, *59*, 1758.
- Perdew, J. P.; Burke, L.; Ernzerhof, M. *Phys. Rev. Lett.* **1996**, *77*, 3865.
- Guest, M. F.; Bush, I. J.; van Dam, H. J. J.; Sherwood, P.; Thomas, J. M. H.; van Lenthe, J. H.; Havenith, R. W. A.; Kendrick, J. *Mol. Phys.* **2005**, *103*, 719.
- DALTON, a molecular electronic structure program, Release 2.0(2005), see <http://www.kjemi.uio.no/software/dalton/dalton.html>.
- Frisch, M. J.; Trucks, G. W.; Schlegel, H. B.; Scuseria, G. E.; Robb, M. A.; Cheeseman, J. R.; J. A. Montgomery, J.; Vreven, T.; Kudin, K. N.; Burant, J. C.; Millam, J. M.; Iyengar, S. S.; Tomasi, J.; Barone, V.; Mennucci, B.; Cossi, M.; Scalmani, G.; Rega, N.; Petersson, G. A.; Nakatsuji, H.; Hada, M.; Ehara, M.; Toyota, K.; Fukuda, R.; Hasegawa, J.; Ishida, M.; Nakajima, T.; Honda, Y.; Kitao, O.; Nakai, H.; Klene, M.; Li, X.; Knox, J. E.; Hratchian, H. P.; Cross, J. B.; Bakken, V.; Adamo, C.; Jaramillo, J.; Gomperts, R.; Stratmann, R. E.; Yazyev, O.; Austin, A. J.; Cammi, R.; Pomelli, C.; Ochterski, J. W.; Ayala, P. Y.; Morokuma, K.; Voth, G. A.; Salvador, P.; Dannenberg, J. J.; Zakrzewski, V. G.; Dapprich, S.; Daniels, A. D.; Strain, M. C.; Farkas, O.; Malick, D. K.; Rabuck, A. D.; Raghavachari, K.; Foresman, J. B.; Ortiz, J. V.; Cui, Q.; Baboul, A. G.; Clifford, S.; Cioslowski, J.; Stefanov, B. B.; Liu, G.; Liashenko, A.; Piskorz, P.; Komaromi, I.; Martin, R. L.; Fox, D. J.; Keith, T.; Al-Laham, M. A.; Peng, C. Y.; Nanayakkara, A.; Challacombe, M.; Gill, P. M. W.; Johnson, B.; Chen, W.; Wong, M. W.; Gonzalez, C.; Pople, J. A. Gaussian 03, revision D.01; Gaussian, Inc.: Wallington, CT, 2004.
- de Boer, J. L.; Vos, A. *Acta Crystallogr.* **1972**, *B28*, 835.
- Mukai, K. *Bull. Chem. Soc. Jpn.* **1969**, *42*, 40.